



**HAL**  
open science

## Space-time evolution of a large field of pockmarks in the Bay of Concarneau (NW Brittany)

Agnès Baltzer, Marine Reynaud, Axel Ehrhold, Jérôme Fournier, Céline Cordier, Hélène Clouet

### ► To cite this version:

Agnès Baltzer, Marine Reynaud, Axel Ehrhold, Jérôme Fournier, Céline Cordier, et al.. Space-time evolution of a large field of pockmarks in the Bay of Concarneau (NW Brittany). *Bulletin de la Société Géologique de France*, 2017, 188 (4), pp.23. 10.1051/bsgf/2017191 . hal-02323079

**HAL Id: hal-02323079**

**<https://hal.science/hal-02323079>**

Submitted on 31 Oct 2022

**HAL** is a multi-disciplinary open access archive for the deposit and dissemination of scientific research documents, whether they are published or not. The documents may come from teaching and research institutions in France or abroad, or from public or private research centers.

L'archive ouverte pluridisciplinaire **HAL**, est destinée au dépôt et à la diffusion de documents scientifiques de niveau recherche, publiés ou non, émanant des établissements d'enseignement et de recherche français ou étrangers, des laboratoires publics ou privés.

## Space-time evolution of a large field of pockmarks in the Bay of Concarneau (NW Brittany)

## Évolution spatio-temporelle d'un champ de pockmarks dans la Baie de Concarneau (Nord-Ouest de la Bretagne)

Baltzer Agnès <sup>1,\*</sup>, Reynaud Marine <sup>2</sup>, Ehrhold Axel <sup>3</sup>, Fournier Jérôme <sup>4</sup>, Cordier Céline<sup>5</sup>, Clouet Hélène <sup>1</sup>

<sup>1</sup> Univ Nantes, Lab Geolittomer, CNRS UMR LETG 6554, F-44312 Nantes 3, France.

<sup>2</sup> Ecole Cent Nantes, LEEA, 1 Rue Noe, F-44321 Nantes 3, France.

<sup>3</sup> IFREMER, Lab Geodynam & Enregistrement Sedimentaire, Ctr Bretagne, ZI Pointe Diable, CS 100700, F-29280 Plouzane, France.

<sup>4</sup> CNRS, Museum Natl Hist Nat, Stn Biol Marine, UMR BOREA 7208, PI Croix, BP 225, F-29182 Concarneau, France.

<sup>5</sup> Laboratoire d'Ecologie Benthique Côtière, centre Bretagne, ZI de la Pointe du Diable, CS 100700, 29280 Plouzané, France.

\* Corresponding author : Agnès Baltzer, email address : [agnes.baltzer@univ-nantes.fr](mailto:agnes.baltzer@univ-nantes.fr)

### Abstract :

About a decade ago, a large field of pockmarks, covering an overall area of 36 km<sup>2</sup> was discovered in water depths of < 30m in the central part of the Bay of Concarneau (Southern Brittany, France). This field, composed of features from 5 m to 35 m in diameter and < 1 m in depth, is characterized by unusual high densities of pockmarks, up to 5840 per square kilometre. Geophysical data correlated with sedimentary samples acquired in 2005 and 2009 show that pockmarks and their immediate surroundings are associated with dense tubes benches cover, built by a filter-feeding amphipod: *Haploopsis nira*, forming original benthic communities. Two complementary surveys were carried out in April 2011 (Pock and Ploops) and April 2014 (Pock and Tide), on the Oceanographic Vedette (O/V) *Haliotis* (Ifremer/Genavir), to map the limit of the pockmarks and *Haploopsis* fields with the maximum accuracy. The link between the presence of the *Haploopsis nira* communities and the occurrence of pockmarks / gas was then established and the proposed hypothesis was that tidal cycles may provide a good candidate for a short-term (monthly) triggering mechanism of fluid expulsion (Baltzer A, Ehrhold A, Rigolet C, Souron A, Cordier C, Clouet H. 2014. Geophysical exploration of an active pockmark field in the Bay of Concarneau, southern Brittany, and implications for resident suspension feeders. *Geo-Marine Letters*, 34, 215-230). Due to the high-level precision (50 cm) of the positioning system (Magellan Aquarius Ixsea Hydrins) coupled with the RTK attitude system, these new bathymetric and imagery maps together with the sub-bottom Chirp profiles, allow us to compare the data sets from April 2011 and April 2014. The superimposition of the two data sets shows that the distribution of the

pockmarks remains similar between these 2 dates (i.e. for 3 years), for the group of large, widely scattered pockmarks, which are deeply rooted in the Holocene palaeo-valley infills and for the group of pockmarks identified as the trawl-scour pockmarks, initiated by trawling action. Most of the pockmarks present very recent shapes without any infilling but sonar imagery reveals that some of them have been covered by a thin muddy layer, thereby reflecting, at least, a temporary cessation of expulsion or a different activity. Chirp profiles indicate some acoustic flares above the pockmarks, revealing gas/fluid expulsion. Different gas clues within the sedimentary column, such as acoustic turbidity, enhanced gas reflectors (EGR), chimneys pipes, occur at exactly the same places on the chirp seismic profiles from 2011 and 2014. Therefore, contrary to most examples described in the literature, this pockmarks field is still active.

## Résumé

Un large champs de pockmarks, couvrant une surface de 36 km<sup>2</sup>, a été découvert il y a une dizaine d'années, dans la partie centrale de la Baie de Concarneau (Bretagne sud, France), par moins de 30 m de fond. Ce champs de pockmarks, composé de cratères mesurant de 10 à 30 m de diamètre pour des profondeurs de 1 m maximum est caractérisé par une densité exceptionnelle, atteignant jusqu'à 5840 structures par km<sup>2</sup>. Des données géophysiques, corrélées et complétées par des prélèvements sédimentaires entre 2005 et 2009, ont montré que ce champs de pockmarks est associé à la présence de colonies de *Haploops nirae*, petit amphipode filtreur benthique, habitant dans des tubes fixés sur le fond et formant de larges banquettes. Deux campagnes complémentaires ont été réalisées en Avril 2011 (Pock and Ploops) et Avril 2014 (Pock and Tide), sur la vedette océnographique Haliotis (Ifremer/Génavir), afin de cartographier très précisément la limite des champs de *Haploops* et des pockmarks. Le lien constaté (mais non élucidé) de la présence des colonies de *Haploops* et de ces pockmarks implique une activité répétée des pockmarks, et la marée comme facteur déclenchant à court terme constitue l'hypothèse la plus robuste (Baltzer A, Ehrhold A, Rigolet C, Souron A, Cordier C, Clouet H. 2014. Geophysical exploration of an active pockmark field in the Bay of Concarneau, southern Brittany, and implications for resident suspension feeders. *Geo-Marine Letters*, 34, 215–230). Grâce au système de positionnement RTK, les données d'imagerie, de bathymétrie et de l'échosondeur à sédiments (chirp) ont pu être parfaitement superposées et donc comparées entre 2011 et 2014. Les premiers résultats montrent que la répartition des pockmarks reste similaire entre ces 2 dates pour le groupe de grands pockmarks dispersés, enracinés plus profondément dans le remplissage sédimentaire holocène des paléo-vallées et le groupe de pockmarks plus petits, plus denses, alignés le long des traces de chaluts de pêcheurs. La plupart des pockmarks présente des cratères sans remplissage sédimentaire, bien qu'il existe dans certains, un fin drappage de vase révélé par l'imagerie sonar, reflétant des arrêts temporaires de l'activité d'expulsion des fluides ou bien un fonctionnement différent. Les profils chirp montrent également des panaches dans la colonne d'eau, indiquant de probables expulsions de fluides/gaz. Plusieurs indices de la présence de gaz sont systématiquement visibles dans la colonne sédimentaire, tels que "la turbidité acoustique", les "réflecteurs acoustiques marqués", les "chimneys pipes". Ainsi, contrairement à beaucoup d'exemples cités dans la littérature, ce champs de pockmarks est encore actif.

**Keywords** : geophysics, pockmarks, tide, turbidity, gas, chimneys pipes, Concarneau

**Mots clés** : géophysique ; marée ; failles ; gaz

74 **Introduction**

75 Pockmarks are crater-like features found on the seabed, which occur in deep marine environments  
76 (King and MacLean 1970; Josenhans et al. 1978; Fader 1991) in lakes, shallow bays, estuaries and  
77 fjords (Hovland and Judd 1988; Kelley et al. 1994; Rogers et al. 2006). They may be classified  
78 according to three criteria: (1) their morphology: circular, elliptical, asymmetrical, composite  
79 (Hovland and Judd 1988; Judd and Hovland 2007); (2) their state of development: new, growing,  
80 decaying (Pickrill 1993); and (3) their mechanisms of formation: e.g. fault-strike pockmarks, iceberg-  
81 scour pockmarks, current modified pockmarks (Pilcher and Argent 2007). They can also be induced  
82 by anthropogenic activities such as trawling and ship anchoring (Harrington 1985; Fader 1991). They  
83 often form in muddy sediments, large deltas, around small basins and along irregular topographic  
84 highs (Hovland and Judd 2009). Deep sources exist for thermogenic hydrocarbons or gas hydrates

85 (Scanlon and Knebel 1989; Rogers et al. 2006; Miller et al. 2015), but they may be related to pore  
86 water expulsion by compaction (Harrington 1985) or may develop above buried paleo-channels that  
87 are rich sources of organic material (Gay et al. 2006; Pilcher et al. 2017; Leon et al. 2009; Leon et al.  
88 2014). However, as active fluid flux is rarely observed in pockmarks, the trigger mechanisms can be  
89 difficult to identify and may result from natural disasters (earthquakes, tsunamis, storms) or occur  
90 more continuously over longer-term events (Kelley et al. 1994; Hovland et al. 2002). Judd and  
91 Hovland (2009) hypothesized that most pockmarks discovered are most of the time inactive, which  
92 was confirmed by Brothers et al. (2012). This paper presents the results of a study conducted on a field  
93 of shallow-water pockmarks (< 30 m of water depth) located in the eastern part of the Bay of  
94 Concarneau, Southern Brittany, France (Ehrhold et al. 2006; Baltzer et al. 2014; Reynaud and Baltzer.  
95 2014). This area is characterised by a high density of pockmarks (an average of 3500 structures/km<sup>2</sup>)  
96 associated with dense *Haploops* tube benches covering muddy environments. The limits of the  
97 pockmark field coincide with the expansion of the *Haploops* communities (Souron 2009), revealing  
98 specific link(s) between them. Reynaud et al. (2014) proposed 3 hypotheses for this link, a food link, a  
99 constructional link (fine sediments supplied by re-suspension is used for tubes building) or a  
100 reproduction/dispersion link (the pockmark activity may keep the larvae inside a limited area with  
101 specific geochemical conditions. Each of these links supposed that pockmarks are active, at least  
102 sometimes.

103 In order to explore the potential activity of this pockmark field, this paper presents the results of two  
104 surveys, Pock and Ploops (2011) and Ploops and Tide (2014), conducted at the same season (April),  
105 and using the interferometric sidescan sonar (I2S) and chirp tools of the O/V Haliotis, characterised by  
106 a very accurate positioning system, coupled to a RTK beacon. Thus it was possible to compare the  
107 state and the space-time evolution of this pockmark field between April 2011 and April 2014 using  
108 these high-level resolution tools. The analyses of the data sets from 2014 allow to determine the  
109 evolution of the acoustic clues of ascending gas, such as blank columns and gas chimneys, and thus  
110 will indicate the state of the vertical connections between the sources and the pockmarks (surface gas  
111 expression) over a 3 year time-frame. These observations better constrain the gas availability of the  
112 system and eventually provide some clues for the preferential pathways used for gas recharge and gas

113 expulsion. The only known fact is that gas is biogenic methane (Baltzer et al. 2014; Dubois et al.  
114 2015). The questions addressed here are: 1) Is there a continuous activity for these pockmarks? 2) If  
115 not, what is the rhythm of expulsion? 3) Where does the gas come from?

116

## 117 **1 General setting**

118 Situated in Southern Brittany (Fig. 1), the Bay of Concarneau covers an area of approximately  
119 200 km<sup>2</sup> above the 50 m isobath. It corresponds to a tectonic depression with a width of 5-6 km and a  
120 length of about 15 km. The bay is bounded by major structural features associated with the Kerform  
121 fault system (N160) (Béchenec et al. 1997) which controls the incised valley of Concarneau (Proust  
122 et al. 2001). Middle Eocene sandstone and calcareous formation unconformably overlap the crystalline  
123 basement rocks. These Eocene series (e 5-6), faulted and folded, are incised by paleo-valleys that  
124 preserve sparse marine calcareous infillings of the upper Oligocene (Bouysse et al. 1974). Two paleo-  
125 valley systems, oriented N120, parallel to the south Armorican fault system and N160 (Kerform  
126 system) respectively, were deepened from the end of the Eocene to the beginning of the Oligocene  
127 (Pinot 1974). These relatively narrow and sinuous palaeo-valleys (200-500 m in width for lengths of  
128 20 and 18 km) converge to form a large and unique drainage system (4 km wide) in the South of the  
129 Pointe de Trévignon (Fig. 2). Fluvial and estuarine pleistocene deposits infill this drainage system.  
130 An holocene sedimentary layer, characterised by a thickness of 3 to 5 m, covers the entire area  
131 (Menier 2003), except for some plateaus like the Maërl Terrasse between Concarneau and Trévignon  
132 (Ehrhold et al. 2006).

133 The hydrodynamic conditions of the study area are characterized by their close dependence on the  
134 geomorphological context. The strongest swells are generally associated with westerly gales. To the  
135 South of Belle-Ile, waves are of a height ranging from 4 to 6 m (Hs), a mean period of 6 to 8 s<sup>-1</sup>, and  
136 mainly come from the W-NW (Tessier 2006). The Bay of Concarneau is relatively protected from  
137 swell dynamics, due to the presence of shallow waters and rocky platforms like the Pourceaux, and the  
138 Glénan Islands (Pinot 1974). The tide is semi-diurnal with a range of 5.5 m for a tidal coefficient of  
139 120. Tidal currents are moderate with a mean value of 0.25 m/s<sup>-1</sup>, integrated on the water column, for a  
140 tidal coefficient of 90 (unpublished data from P. Bailly du Bois, IRSN). Surface currents can reach a

141 velocity of  $15 - 30 \text{ cm/s}^{-1}$  whereas under-water velocities range from  $0 - 5 \text{ cm/s}^{-1}$  for a coefficient of  
142 100 (Tessier 2006). Tidal currents describe a clock wise movement, from South to South-West during  
143 ebb to North to North-East during floods. Locally, the intensity of the current is lower than  $30 \text{ cm/s}^{-1}$   
144 between Concarneau and Trévignon.

145

## 146 **2 Data and methods**

### 147 2-1 Acoustic measurements acquisition

148

149 The data used in this study is the result of two oceanographic sea surveys. The Pock and Ploops survey  
150 was conducted in April 2011 aboard the Oceanographiv Vedette O/V Haliotis (Ifremer/Génavir). This  
151 vessel is equipped with a hull-mounted interferometric sonar (GeoAcoustics GeoSwath, 250 kHz)  
152 which allowed simultaneous acquisition of bathymetric and sonar images. 1250 km of profiles were  
153 acquired, with 96 profiles obtained in four non-contiguous areas, area 1, area 2, area 3, area 4 (Fig. 1  
154 & 2). The Pock and Tide survey in April 2014 aboard the O/V Haliotis complemented the 2011 data  
155 set with the acquisition of 205 additional profiles (shaded lines on figure. 1); additionally, some  
156 profiles acquired in 2011 were exactly replicated in 2014 (shaded lines within the areas 1, 2, 3 and 4  
157 on figure 1).

158

### 159 2-2 Acoustic measurements processing

160

161 The 2011 and 2014 survey sidescan sonar data was processed with GeoTexture (GeoAcoustic) and  
162 bathymetry data with CARAIBES software, developed by Ifremer. The bathymetric and sidescan  
163 sonar resolutions are respectively 80 and 50 cm. This acoustic data was exported and interpreted in  
164 ESRI ArcGIS. Sidescan sonar data gives a picture of acoustic backscatter properties of the seabed  
165 which is illustrated by a grayscale image (Augustin et al. 1994). Acoustic backscatter varies depending  
166 on the angle of incidence of the acoustic wave front to the seabed, the impedance contrast across the  
167 sediment-water interface, surface roughness, and bathymetry and volume reverberation. Grey tones of  
168 the sonar image will depend on the nature and the compaction of the sediment, as well as on the

169 topography of the seabed. Light tones generally represent low backscatter, such as relatively finer-  
170 grained and underconsolidated sediments and dark tones represent high backscatter, such as relatively  
171 coarser-grained or compacted sediments, while a high slope gradient will appear darker. Seventeen  
172 Shipeck core boxes were sampled during the second survey to identify and confirm the *Haploops*  
173 acoustic facies on sonar images.

174 The picking of the pockmarks was realised manually, on ArcGIS (Reynaud and Baltzer, 2014)  
175 providing an accurate map (resolution of 50 cm) of the pockmark distribution. Tidal corrections and  
176 centimeter precision positioning of data were made possible thanks to an Aquarius Thalès GPS, an  
177 RTK beacon located on the coast and a tide-gauge-buoy.

178

### 179 **3 Results**

#### 180 3-1 Bathymetry maps

181

182 For each of the areas (large black frame), of the bathymetry map, 1 focus zone (small white frame)  
183 was selected within areas that were surveyed both in 2011 and 2014 (Fig.1). The global bathymetry  
184 map, grouping data from 2011 and 2014 acquisitions, is shown on Figure 2. The exceptional density of  
185 the pockmarks (5 840 features/km<sup>2</sup>) is much higher than the usual descriptions found in the literature  
186 (Garcia-Garcia et al. 1999; Ferrin et al. 2003). Presenting a sub-circular to circular shape, in particular  
187 aalong the palaeo-valleys, and the diameter of the pockmarks varies from 5 m (exceptionnally less  
188 than 1 m-limit of the sonar resolution) to 35 m with only a few decimetres in depth. Pockmark depths  
189 are difficult to measure as chirp profiles do not often exactly pass through pockmarks. The  
190 comparison of bathymetry sets for the 4 focus zones (Fig. 3) clearly shows that almost all the  
191 pockmarks occurred at the same location in 2011 and 2014, without any substantial change between  
192 these two dates, except a trend towards more marked features in 2014. This may be explained by the  
193 data processing : the same resolution was used for both dates but not the same colour code, which  
194 explains the different aspect of the 2011 maps (Fig. 3). On all the focus zones, the global distribution  
195 remain similar with some very few changes in pockmarks locations: the black circle or oval covers the  
196 same area sample, and reveals a new pockmark distribution



197 On focus 1, trawl-scour pockmarks appear, perfectly visible and aligned, in 2011 and in 2014.  
198 On focus 2, a third pockmark seems to have occurred in the right circle, and two pockmarks appear  
199 more marked in the black oval, on the left.  
200 On focus 3, a new pockmark occurred in 2014, underlined by the circle on the right (Fig. 3).  
201 On focus 4, the black circle on the right designates the occurrence of new pockmarks.  
202 Eventually, Focus 5 shows an extract of the bathymetry acquired in 2011 (location on Figure 2), where  
203 it is possible to distinguish small pockmarks (around 8 meters), large pockmarks (around 25 meters)  
204 and within the large ones, some deeper pockmarks (alpha type), with a net crater shape or shallower  
205 pockmarks (beta type) with a smoothy crater shape.

206

### 207 3-2 Sidescan imagery

208

209 Sidescan imagery has revealed that the limits of the settlements of *Haploops* colonies (Fig. 2) coincide  
210 with the presence of a field (36 km<sup>2</sup>) of pockmarks (Baltzer et al. 2014). This field extends to the  
211 South of Trévignon, up to the north-east of the Glénan Islands (Fig. 2). The main result of the  
212 comparison of the sonar images from 2014, confirmed by direct-field observations with scuba-diving,  
213 is that the distribution of the *Haploops* colonies is related to the pockmark field limits all around the  
214 studied area. To the south, tubes benches have become discontinuous and have begun to be more and  
215 more fragmented, to finally disappear just after the pockmark field boundaries (Ehrhold et al. 2006;  
216 Baltzer et al. 2014)

217 The comparison of the two sonar mosaics reveals that for some pockmarks, located along the east edge  
218 of the area 2, there is some thin layer of mud deposit in 2014 which was not there in 2011.

219

### 220 3-3 Seismic profiles

221

222 A total of 98 seismic chirp profiles were acquired during the sea surveys realised in 2011 in 4 areas  
223 (Fig. 1 & Fig. 2), and 205 profiles were acquired in 2014 to complete the survey. In each area, some  
224 profiles acquired in 2011 were exactly replicated in 2014. Figures 4, 5, 6 and 7 present one

225 characteristic profile realised for each area. The sedimentary infilling of the Bay of Concarneau has  
226 been studied for decades and the interpretation is based on the four seismic units described by [Menier](#)  
227 [\(2003\)](#) and used by [Baltzer et al. \(2014\)](#). Above the bedrock composed of paleozoic granite and  
228 oligocene sandy limestone (Unit 0), three seismic units infill the incised palaeo-valley (Figs. 4, 5, 6, &  
229 7). Unit 1, not observed in the area because of gas occurrence, is a relict unit, only preserved as  
230 patches in the deepest parts of the valley, correlated to braided fluvial sediments aged from middle  
231 Pleistocene by [Laurent \(1993\)](#),.. Unit 2 is composed of low amplitude flat parallel reflectors, which  
232 onlap the valley sides and locally downlap the base unit, interpreted as inner mud flat facies. Unit 3  
233 occurs above Unit 2 and presents a surface characterised by a smooth sided U-shaped channel. The top  
234 of this Unit corresponds to an erosional surface and represents tidal flat deposits with coarser lag  
235 deposits within tidal channels. Unit 4 extends over the whole of the valley system, except on the  
236 terrace situated between Concarneau and Trévignon, which is covered by rocky shoals and maerl beds  
237 (Fig. 2) ([Ehrhold et al. 2007](#)). Most of this unit is composed of flat-bedded aggrading deposits,  
238 characterised by low seismic amplitude reflectors and corresponds to unconsolidated Holocene muds,  
239 rich in turritelids ([Bouysse et al. 1974](#); [Ehrhold et al. 2006](#)).

240

241 The limits of the pockmark field correspond to the lateral extension of seismic Unit 3 ([Baltzer et al.](#)  
242 [2014](#)). This unit is cut by different acoustic anomalies, called “acoustic turbidity”, “acoustic blanket”,  
243 “acoustic curtain”, “acoustic column” or “pillar shaped” and chimney pipes depending on their lateral  
244 extension, ([Hovland and Judd 1988](#); [Garcia-Gil 2002](#); [Baltzer et al. 2005](#); [Akulichev et al. 2015](#)).

245 While the pockmark distribution is related to the existence of Unit 3, the size of the pockmarks tends  
246 to correspond to the thickness of this unit. The small pockmarks are correlated with a maximum  
247 thickness of 3 ms (4,5m) for Unit 3, with a gassy reflector situated around 2 ms (1,5m) below the  
248 seabed. The larger pockmarks correspond to a thickness of up to 12 ms (9 m) for Unit 3, with a gassy  
249 reflector observed from 4 ms (3,5 m) to 8 ms (6 m). Within this large pockmark group, some of them  
250 appear to be aligned along the palaeo-valley edges, related to the sedimentary infilling of these paleo-  
251 valleys ([Baltzer et al. 2014](#)).

252

253 Figure 4 presents profile 82 (2011) and profile 72 (2014), revealing 3 branches of the palaeo-river  
254 along the Kerforne fault (Fig. 3). Gas facies occur in the two eastern branches and cross through units  
255 2 and 3 up to the surface. The seabed surface corresponds to a serrated (saw-shaped) reflector, due to  
256 the presence of *Haploops* tubes and pockmarks, clearly visible between shots 400 and 1600. It is  
257 framed by a continuous sea bottom reflector, with no *Haploops* benches, visible from shot 0 to 100  
258 and from 1650 to 2100. Profile 72, (the poor quality is due to the weather), shows that gas was still  
259 present in 2014, confined exactly to the same places, reaching the surface via the same acoustic  
260 columns.

261 Figure 5 shows profiles 68 (2011) and 32 (2014) which cross the Kerforne paleo-valley and the  
262 western branch (Fig. 3). Bench tubes colonize the whole seabed surface (serrated seabed reflector)  
263 and some large pockmarks occur above the main palaeo-valley, especially along the valley edges,  
264 connected to the gas ascension seen in the acoustic columns or chimney pipes. The blanket acoustic  
265 facies correspond to the infilling of the western branch, characterized by smaller pockmarks issued  
266 from the interfluvium. The same pathways crossing units 2 and 3 were used, with three chimney pipes  
267 (red circles) reaching the seabed.

268 Figure 6 reveals large pockmarks on the surface connected with subjacent acoustic blanket facies. The  
269 seabed topography underlines the interfluvium between the palaeo-valleys. The top of Unit 2 presents a  
270 discontinuous surface, slightly hummocky, with large and irregular depressions. These depressions are  
271 connected with the acoustic blanket underneath and resemble to the actual surface pockmarks, but  
272 larger in size. Note that the density of surface pockmarks reflects the proximity of the sub-bottom  
273 gas blanket.

274 Figure 7 shows a clear bulge corresponding to the actual interfluvium superimposed on a paleo bulge,  
275 together with depressions (similar to large pockmarks?). The occurrence of large pockmarks on the  
276 left part of the bulge seems to be related to the presence of a gas “diapir”, which is connected to  
277 reflectors underneath. Does this reflector represent a preferential conduit for gas circulation, down-  
278 lapping the bulge? Each time gas is close to the surface, large pockmarks occur.

279 All the seismic profiles, within each of the different areas, present very similar profiles in 2011 and  
280 2014, with the same visible gas column ascension pathways (chimney pipes), occurring at the same  
281 places with the same connections to the surface towards the pockmark features.

282

283

## 284 **Discussion**

285

286 The first question is whether these pockmarks are still active, just dormant or fossil features? [Judd and](#)  
287 [Hovland \(2007\)](#) hypothesized that most pockmarks discovered are indeed inactive and [Brothers et al.](#)  
288 [\(2011\), \(2013\)](#) have shown that pockmarks may be self-scouring features after initial formation.

289 In the Concarneau's pockmarks field, bathymetry maps show that most of the pockmarks seem to be  
290 empty craters like the pockmark Alpha (Fig. 3 – Focus 5), except some pockmarks with unclear crater  
291 limits like the pockmark Beta (Fig. 3 – focus 5). Reflectivity images present white backscattering  
292 inside some of these pockmarks, attesting that they are infilled with muddy deposits, whereas most of  
293 them appear to be free of infilling ([Ehrhold et al. 2006; Souron 2009](#)). Video images confirm the  
294 presence of fluid mud inside some pockmarks, whereas most of them are empty and surrounded by  
295 *Haploops* colonies ([Reynaud and Baltzer 2014](#)). The occurrence of several “flares” on the chirp  
296 profiles (Figs. 4, 5 and 6) together with flares observed in the water column during mid-current  
297 flowing tides for spring tides ([Baltzer et al. 2014](#)) indicate the activity of, at least, some pockmarks.  
298 Moreover, turbidity was observed by divers during 2011 explorations for biologists works ([Dubois et](#)  
299 [al., 2015](#)) and significant turbidity was observed in the global area in summer 2015 during a SHOM  
300 (Service Hydrographique et Océanographique de la Marine) oceanographic cruise (com. pers. from E.  
301 Marshes). Two more direct observations tend to confirm the activity of this pockmark field: 1) the  
302 persistence of “nude” pockmarks, without any haploops tubes inside, in contrast to the density of the  
303 surrounding colonies and 2) the existence of fragmented tubes in some pockmarks, revealing recent  
304 gas/fluid expulsion. All these arguments attest the presence of active pockmarks in this field but with a  
305 discontinuous activity. Eventually, the presence itself of *Haploops* settlements confirm this  
306 observation.

307 Thus, the second question addressed here where does the gas come from ?  
308 Chirp profiles analyses have highlighted the availability and depth of gas sources (Baltzer et al. 2014),  
309 which will, in turn, control the pockmark distribution. Then, the pockmark distribution on the seabed  
310 represents the spatial arrangement of individual upward-seepage drainage-conduits connected to the  
311 deeper sediment layers and sources. Gas migration and seepage to the surface are usually related to the  
312 existence of two geological features, a gas migration source and a preferential route for gas motion  
313 (fewer resistance pathways). The comparison of the data sets of 2011 and 2014 reveals that the global  
314 distribution of the pockmarks remains similar, and that only a few new pockmarks occurred in 2014.  
315 The permanence of this pockmark pattern observed in the 2014 bathymetry (Fig. 3) tend to attest the  
316 presence of permanent preferential pathways.

317 Chirp profiles show these preferential pathways, revealed by enhanced reflectors and chimneys pipes  
318 (Figs. 4, 5, 6 and 7). Moreover, the comparison of the chirp profiles, from April 2011 to April 2014,  
319 revealed that the gas pathways occurred at the same depth, in the same location, without any or very  
320 few vertical or horizontal fluctuations. This observation confirms the stability of the system which  
321 supplies, at least for 3 years, gas from palaeo-valley floor sources to the surface.

322 The distribution of the pockmarks related to the palaeo-valleys is in agreement with several scientific  
323 papers (Garcia-Gil et al. 2002; Ussler et al. 2003; Rogers et al. 2006; Brothers et al. 2012;  
324 Weschenfelder et al. 2016 ). Enhanced Gas Reflector identified on chirp profiles (Fig. 4, 5, 6 and 7)  
325 correspond to gassy sediment levels issued from biogenic gas, methane (Baltzer et al. 2014; Dubois et  
326 al. 2015), generated by bacterial activity buried under a few metres in sediment rich in organic matter  
327 along the paleo rivers (at least 7% from Floodgate and Judd (1992); Garcia-Gil et al. (2002). Different  
328 authors describe such gassy sediment levels at the Pleistocene/Holocene interface (Chronis et al. 1991;  
329 Gontz et al, 2002; Weshenfelder et al. 2016) as being related to the significant organic matter  
330 degradation in the infilling transgressive deposits, sealed by thin Holocene muds. The combination of  
331 the permeability of this sealing layer and its resistance to stress build-up controls the rate of gas/fluid  
332 leakage from the reservoir to the surface. Once the upward pressure decreases, a pockmark will form  
333 a circular shape. Cathles et al. (2011) have shown that when a gas chimney reaches halfway from the  
334 reservoir to the seabed, liquefaction of overlaying sediments initiate pockmark formation. Kluesner et

335 [al. \(2013\)](#) shows that gas migrates upwards through conduits (e.g. faults) and intra sedimentary  
336 discontinuities, along the valley edges, (e.g. until gas is blocked by a sealing layer). The figure 8  
337 shows on the left-hand side, the pockmark distribution obtained by hand made plotting ([Reynaud and](#)  
338 [Baltzer, 2014](#)). On the right-hand side, the superimposition of the pockmark density map with the  
339 geological BRGM map, shows that the limits of the pockmark field is restricted almost exactly to the  
340 eocene calcareous outcrop in (e 5-6), a nummulitic limestone (Lutetian to Bartonian age). This  
341 formation is strongly faulted, faults belonging to the Kerforne faults system, and underlined by black  
342 lines on the Figure 8. The pockmark density appears to be exceptional, with densities up to 5840  
343 features/ km<sup>2</sup>, when faults are combined with the presence of palaeo-valleys junctions. Patches  
344 without any (or very few) pockmarks (<290) do not show specific distribution, probably related to the  
345 sedimentary cover itself and the different permeability and resistance to stress of the intrasedimentary  
346 sealing layer. Thus, the preferential pathways supplying large pockmarks, situated along the palaeo-  
347 valley edges and within the palaeo-valley infilling itself, were initiated during seismic events which  
348 have shaken the faulted Eocene, creating migration pathways into the sedimentary column (U2,  
349 U3,U4) for escaping methane. [Cathles et al. \(2010\)](#) pointed out that once a pockmark forms, depletion  
350 of the gas reserve can occur as quickly as within one year. After this period, the pockmark will  
351 become dormant and during dormancy, shallow gas reservoirs can recharge. [Judd and Hovland \(2007\)](#)  
352 noted that vertical stacking of pockmarks in seismic data points to episodic reoccurrence of discharge.  
353

354 Then, the last question is related to the dormancy period of the pockmarks of Concarneau and the  
355 rhythm of the gas/fluid/ expulsion. [Baltzer et al., \(2014\)](#) proposed as triggering mechanisms that short  
356 term pressure controlled by the tide could be superimposed on longer term temperature controlled  
357 processes and episodically on earthquake occurrence.

358 The results presented in this paper reveal that pockmarks activity is discontinuous but sufficiently  
359 frequent to keep chimneys pipes and intra sedimentary pathways permanent (visible) for 3 years into  
360 the sedimentary columns. Combining these observations, two models are proposed in Figure 9,  
361 illustrating two cases: the “bottom-up” and the “top-down” preferential pathways for gas migration.

362 The first one illustrates the natural migration of the gas stored in the valley sedimentary infilling,  
363 through the units U2, U3, and U4 and the second one shows the anthropogenic induced migration,  
364 through the trawl-scours pathways. For both models, the gas (biogenic methane) is issued from the  
365 bottom of a paleo-valley, deep enough to allow the maturation of buried organic matter. If the  
366 thickness of the sedimentary infilling is not sufficient (palaeo-valley on the left of the block diagram),  
367 there is no clue of any gas discharge (no pockmarks).

368 The “bottom-up” model supposes that the initial pockmark craters were formed during seismic events  
369 which have shaken the faulted Eocene, creating preferential pathways in the sedimentary column (U2,  
370 U3,U4). The shifting of the gas horizon (EGR), materialised by red arrows on Figure 9, illustrates the  
371 shifting of methane solubility due to the spring tidal pressure (Diez et al. 2007). This shifting would  
372 enable the gas horizon (EGR) to reach the chimneys pipes, possibly at different levels, like at the base  
373 of estuarine muds of U3 or at the base of intercalated storm deposits of U4. Thus, each time the tidal  
374 pressure is high enough, during spring tides or storms, the tidal pumping effect connects the “bottom-  
375 up” pathways to the chimney pipes and pockmarks are re-activated: flares may be observed in the  
376 water column.

377 The “top-down” model illustrates the case of a preferential pathway originated from the seafloor and  
378 descending to reach the gaz horizon (ENG). In this case, these preferential patways have been created  
379 by the trawling action and result in trawl-scour pockmarks, a process similar to the iceberg-scour  
380 pockmarks one . As for the first model, the connection is realised and the pockmark is active when  
381 spring tide overpressure is sufficient.

382

383 These observations give an intermittent pattern of pockmarks activity, which will be a function of the  
384 EGR depth, the water depth and the tidal (or storms) overpressure conditions. The proposed  
385 hypothesis is that during each spring tide, some permanent pockmarks are re-activated, depending on  
386 their water depth and the spring tide coefficient. New pockmarks may be created only during storms or  
387 earthquake events, which would explain their small numer.

388

389 These observations imply that the quantity of gas supplied in the water column may be substantial and  
390 that the gas recharge is continuous. Such observations were made by [Hasiotis et al. \(1996\)](#) who  
391 described such acoustic turbidity in the Gulf of Patras and suggested that there is a continuous supply  
392 of gas towards the pockmarks from below, and that the sediments within the migration path are loaded  
393 with gas.

394 To undertake further study in this area, the objective will be to record gas/fluid expulsion in the water  
395 column, and to understand the rhythm of these expulsions. To do so, one long piezometer and a  
396 special monitoring tool for gas/fluids and turbidity measurements (from SHOM/IFREMER), will be  
397 implanted for longer term observations in this pockmark field.

398

### 399 **Conclusion**

400 The pockmarks of the Bay of Concarneau appear to be active, probably due to combined trigger  
401 processes occurring at different time scales. Earthquake movement (common in this area) may be  
402 relayed or added to short-term controlled tidal pressure (spring tide) processes, thereby triggering gas  
403 escape along preferential pathways. These pockmarks are connected to the paleo-valley infillings,  
404 along intra-sedimentary and structural discontinuities, continuously supplying gas to the upper  
405 sedimentary layer. The expulsion process is activated when connection between the gas horizon  
406 (ENG) and preferential pathways is realised. This system appears to be stable, at least for a short time  
407 scale (decades) revealed by the constant distribution of pockmarks. An intermittent regular pattern of  
408 expulsions is proposed here, which is function of the tidal overpressure, the water depth, and the depth  
409 of the ENG. It is suggested that exceptional overpressure induced by storms or earthquakes may  
410 create new pockmarks. Nevertheless, the rhythm of expulsion together with the nature itself of the  
411 expelled gas/fluid need to be explored. Future work will focus on the above water column study with  
412 the implantation during at least 6 months of a camera and a piezometer. This next research project will  
413 allow the measurement of the volume of gas produced and injected into the water column of this bay.

414

### 415 **Acknowledgements**



416 Special thanks are due to the captains of the Oceanographic Vedette Haliotis Arnaud Gillet and the  
417 informatic engineer Renaud Cagna. The first sea survey (2011) was partly funded by the Total  
418 Foundation for Biodiversity and the Sea in the framework of an IFREMER/TOTAL project. This  
419 article benefitted from rich and constructive feedback from the two reviewers.

420

421

422 **Figure captions:**

423

424 **Figure 1:** Location of the profiles acquired during the two oceanographic sea surveys realised with the  
425 O/V Haliotis in 2011 (Pock and Ploops) and 2014 (Pock and Tide) between Concarneau estuary,  
426 Trevignon spur and Glénan Islands. For each profile, bathymetric, sonar images and chirp data have  
427 been acquired. Four areas were delimited (black frames) during the 2011 sea survey and were  
428 completed during the 2014 sea survey (dashed grey lines). White frames delimit 5 focus zones. For  
429 focus zones 1, 2, 3 and 4, profiles were renewed in 2014 (figure 2). The black line limits the extension  
430 of the *Haploops nirae* mats.

431

432 **Figure 2:** Bathymetric map of the area compiled from data acquired in 2011 and 2014. Palaeo-valleys,  
433 determined from chirp profiles, have been superimposed on the map (dark blue). Red lines show the  
434 location of the profiles selected in figures 4, 5, 6 and 7.

435 The white line represents the Haploops area limits: it has been drawn on the side scan imagery, where  
436 black grey facies corresponds to *Haploops* tubes (see photos) and light grey facies corresponds to mud  
437 with no *Haploops* tubes present. The white frames represent the focus zones from 1 to 5.

438

439 **Figure 3:** For Focus 1, Focus 2, Focus 3 and Focus 4 zones, (white frames in figure 1), an extraction  
440 of bathymetric maps was realised in 2011 and 2014. The comparison of the two bathymetric  
441 extractions reveals the almost perfect superimposition of pockmarks from 2014 and 2011. Focus 5  
442 shows a detailed bathymetry map with large and small pockmarks. Large pockmarks (> 20 m) usually  
443 occur very clearly on the bathymetry, such as the Alpha pockmark indicated, but may sometimes

444 present smoother contours.

445

446 **Figure 4:** Area 1: chirp profile 82 was realised in 2011 and was replicated in 2014 (profile 72), exactly  
447 at the same location (see location on figure 2). Interpretation of Profile 82 reveals the presence of gas  
448 intercalated in the different valley branches. Gas pathways issued from the bottom of the palaeo-  
449 valleys occurred at the same places in 2011 and 2014 (whereas the 2014 data quality is poor, because  
450 of the weather).

451 The sea-bottom reflector appears to be continuous and highly reflective in the absence of *Haploops*  
452 tubes, whereas it presents a serrated shape when *Haploops* tubes are present.

453

454 **Figure 5:** Area 2: chirp profile 68 was realised in 2011 and was replicated in 2014 (profile 32), exactly  
455 at the same location (see location on figure 2). Interpretation of Profile 68 reveals the presence of gas  
456 within the main valley. Gas issued from the bottom of this paleo-valley followed the same pathways in  
457 2011 and 2014, materialised by chimney pipes (red circles), and creating pockmarks (red circles) on  
458 the sea floor. A flare occurs on profile 68, which was not present in 2014.

459

460 **Figure 6:** Area 3: chirp profile 41 was realised in 2011 and was replicated in 2014 (profile 178),  
461 exactly at the same location (see location on figure 2). Interpretation of Profile 41 reveals the presence  
462 of gas within the main valley, and the absence of gas within the small buried valley on the left. There  
463 are no *Haploops* tubes above the small buried valley. Gas issued from the bottom of the paleo-valley  
464 followed the same pathways in 2011 and 2014, materialised by chimney pipes (red circles), and  
465 creating pockmarks on the sea floor surface.

466 **Figure 7:** Area 4: chirp profile 30 was realised in 2011 and was replicated in 2014 (profile 122),  
467 exactly at the same location (see location on figure 2). Interpretation of Profile 30 reveals the presence  
468 of gas within the main valley, and the absence of gas within the small buried valley on the left. There  
469 are no *Haploops* tubes above the small buried valley. Gas issued from the bottom of the paleo-valley  
470 followed the same pathways in 2011 and 2014, materialised by chimney pipes (red circles), and  
471 creating pockmarks on the sea floor surface.

472 .

473 **Figure 8A:** Pockmark distribution merged from 2011 and 2014 data. All the pockmarks have been  
474 manually plotted (resolution of 50 cm).

475

476 **Figure 8B:** Superimposition of the geological map (1:250 000 vectorised map from BRGM) with the  
477 map of pockmark density. The black lines delimit the *Haploops niraë* area. The light brown line  
478 delimits the eocene outcrop (e5-6), coloured in yellow on the geological map. Faults are underlined by  
479 a black line and the paleo-valleys are represented by blue lines.

480

481 **Figure 9:** Two sketches illustrating the possible pathways for gas migration are presented in this  
482 paper: the upper block diagram shows a “bottom-up” model and the second diagram shows a “top-  
483 down” model for gas along preferential pathways.

484 **Figure 9A:** The “bottom-up” model shows the gas, issued from the buried organic matter at the  
485 bottom of the buried valley, migrating along preferential pathways in U2. Gas is stopped and stored  
486 just under the EGR (Enhanced Gas Reflector) at the top of U2. A second network of pathways may  
487 conduct gas through U3 up to the base of U4. Consequently, gas is able to migrate up to the sea floor  
488 surface, via tidal pumping processes, creating the large pockmarks. Note the presence of chimney  
489 pipes within the unit U4.

490

491 **Figure 9B:** The “top-down” model illustrates the specific case of the trawl-scour pockmarks. These  
492 pockmarks have been triggered by the trawls of fishing boats on the sea floor. The digging action  
493 initiates a preferential pathway for gas escape, resembling iceberg-scours.

494 **References**

- 495 AKULICHEV V.A., ASTAKHOV A.S., KARNAUKH V.N., AKSENTOV K.I., ARTEMOVA A.V.,  
496 BOSIN A.A., VERESHCHAGINA O.F., VOLOGINA E.G., IVANOV M.V., KALINCHUK V.V., &  
497 SUKHOVEEV E.N. (2015). - Submarine coaliferous formations to Holocene sediments (Amur Bay,  
498 Sea of Japan). *Doklady Earth Science*, **460**, 163-167.  
499
- 500 AUGUSTIN J.M., EDY C., SAVOYE B., & LEDREZEN E. (1994). - Sonar mosaic computation  
501 from multibeam echosounder. Rapport interne IFREMER, p. 57.  
502
- 503 BALTZER A., TESSIER B., NOUZÉ H., BATES R., MOORE C., & MENIER D. (2005). - Seistec  
504 Seismic Profiles: A Tool to Differentiate Gas Signatures. *Marine Geophysical Research*, **26** (2-4),  
505 235-245.  
506
- 507 BALTZER A., EHROHOLD A., RIGOLET C., SOURON A., CORDIER C., CLOUET H., &  
508 DUBOIS S. (2014). - Geophysical exploration of an active pockmark field in the Bay of Concarneau,  
509 southern Brittany, and implications for resident suspension feeders. *Geo-Marine Letters*, **34**, 215-230.  
510
- 511 BECHENNEC F., GUENNOC P., GUERROT C., LEBRET P., & THIEBLEMONT D. (1997). -  
512 Notice explicative, carte géologique de France, 1/50000 feuille Concarneau (382). BRGM, Orléans.  
513
- 514 BOUYASSE P., CHATEAUNEUF J., & TERS M. (1974). - Présence d'Ypresien, niveau transgressif et  
515 taux de sédimentation flandriens (Bretagne méridionale) en baie de Vilaine. *Comptes-Rendus de*  
516 *l'Académie des Sciences*, Paris, **279**, 1421-1424.  
517
- 518 BROTHERS L.L., KELLEY J.T., BELKNAP D.F., BARNHARDT W.A., ANDREWS B.D., &  
519 MAYNARD M.L. (2011). - More than a century of bathymetric observations and present-day shallow  
520 sediment characterization in Belfast Bay, Maine, USA: implications for pockmark field longevity. *Geo-*  
521 *Marine Letters*, 31, 237-248.

522

523 BROTHERS L.L., KELLEY J.T., BELKNAP D.F., BARNHARDT W.A., ANDREWS B.D., &  
524 LEGERE C. (2012). - Shallow stratigraphic control on pockmark distribution in north temperate  
525 estuaries. *Marine Geology*, **329-331**, 34-45.

526

527 BROTHERS L.L., VAN DOVER C.L., GERMAN C.R., KAISER C.L., YOERGER D.R., RUPPEL  
528 C.D., LOBECKER E., A.D. SKARKE A.D., & WAGNER J.K.S. (2013). - Evidence for extensive  
529 methane venting on the southeastern US Atlantic margin. *Geology* 41, 807–810.

530

531 CATHLES L.M., SU Z., & CHEN D. (2010). - The physics of gas chimney and pockmark formation,  
532 with implications for assessment of seafloor hazards and gas sequestration. *Marine and Petroleum*  
533 *Geology*, **27**(1), 82-91.

534

535 CHRONIS C., PIPER D., & ANAGNOSTOU G. (1991). - Late Quaternary evolution of the Gulf of  
536 Patras. *Marine Geology*, **97**, 191–209.

537

538 DIEZ R., GARCIA-GIL S., DURAN R., & VILAS F. (2007). - Gas accumulations and their  
539 association with particle size distribution patterns in the Ria de Arouza seabed (Galicia, NW Spain) an  
540 application of discriminante analyses. *Geo-marine Letters*, **27** (2/4), 89-102.

541

542 DUBOIS S., DERIAN F., CASEY X., RIGOLET C., CAPRAIS JC., & THIEBAUT E. (2015). – Role  
543 of pockmarks in diversity and species assemblages of coastal macrobenthic communities. *Marine*  
544 *Ecology Progress Series*, **529**, 91-105.

545

546 EHRHOLD A., HAMON D., & GUILLAUMONT B. (2006). - The REBENT monitoring network, a  
547 spatially integrated, acoustic approach to surveying nearshore macrobenthic habitats: application to the  
548 Bay of Concarneau (South Brittany, France). *ICES Journal of Marine Science*, **63**, 1604-1615.

549

550 EHRHOLD A., BLANCHET A., HAMON D., CHEVALIER C., GAFFET J.D., & ALIX A.S. (2007).  
551 - Réseau de surveillance benthique (REBENT) - Région Bretagne. Approche sectorielle subtidale:  
552 identification et caractérisation des habitats benthiques du secteur de Concarneau. Brest, RST Ifremer  
553 Dyneco Ecologie Benthique, p.78.  
554  
555 FADER G.B. J. (1991). - Gas related sedimentary features from the eastern Canadian continent shelf,  
556 *Continental shelf research*, **11**, 1123-1154.  
557  
558 FERRIN A., DURAN R., DIEZ R., GARCIA-GIL S., & VILAS F. (2003). - Shallow gas features in  
559 the Galician Rías Baixas (NW Spain). *Geo-Marine Letters*, **23**, 207–214.  
560  
561 FLOODGATE G.D., & JUDD A.D. (1992). - The origin of shallow gas. *Continental Shelf Research*,  
562 **12**(10), 1145–1156.  
563  
564 FOURNIER J., BALTZER A., GODET L., & PANIZZA A. (2010). - Acoustic imagery for benthic  
565 habitats mapping and monitoring, Chapter 5, in *Geomatic solutions for coastal environments*, Eds. M.  
566 Maanan & M. Robin, Series Environmental Science, Engineering and Technology, Noca Science  
567 Publishers, Inc., New-York, 141-161.  
568  
569 GARCIA-GIL S., VILAS-MARTIN F., MUÑOZ A., ACOSTA J., & UCHUPI E. (2002). -  
570 Quaternary sedimentation and thermal diapirism in the Ria de Pontevedra (Galicia), Northwest Spain.  
571 *Journal of Coastal Research*, **15**(4), 1083–1090.  
572 GARCÍA-GARCÍA A., VILAS F., & GARCÍA-GIL S. (1999). - A seeping sea-floor in a Ria  
573 environment: Ria de Vigo (NW Spain). *Environmental Geology*, **38**(4), 296–300.  
574  
575 GAY A., LOPEZ M., ONDREAS H., CHARLOU J.L., SERMONDADAZ G., & COCHONAT P.  
576 (2006). - Seafloor facies related to upward methane flux within a Giant Pockmark of the Lower Congo  
577 Basin. *Marine Geology*, **226**(1-2), 81-95.

578

579 GONTZ A.M., BELKNAP D.F., & KELLEY J.T. (2002). - Seafloor features and characteristics of the  
580 Black Ledges area, Penobscot Bay, Maine, USA. *Journal of Coastal Research*, **36**, 333 – 339.

581

582 HARRINGTON P.K. (1985). Formation of pockmarks by pore-water escape. *Geo-Marine Letters*, **5**,  
583 193–197.

584

585 HASIOTIS T., PAPTAEODOROU G., KASTANOS N., & FERENTINOS G. (1996). - A pockmark  
586 field in the Patras Gulf (Greece) and its activation during the 14/7/93 seismic event. *Marine Geology*,  
587 **130**, 333 – 344.

588

589 HOVLAND M., & JUDD A. (1988). - Seabed pockmarks and seepages: impact on geology, biology,  
590 and the marine environment. London, Graham and Trotman, p. 293.

591

592 JOSEPHANS H.W., KING L.H., & FADER G.B. (1978). - Side scan sonar mosaic of pockmarks on  
593 Scotian shelf. *Canadian Journal of Earth Sciences*, **15**, 831-840.

594

595 JUDD A.G., & HOVLAND M. (2007). - Seabed Fluid Flow: The Impact on Geology, Biology and the  
596 Marine Environment. Cambridge: Cambridge University Press, p. 492.

597

598 KELLEY J.T., DICKSON S.M., BELKNAP D.F., BARNHARD W.A., & HENDERSON M. (1994). -  
599 Giant seabed pockmarks evidence for gas escape from Belfast Bay, Maine. *Geology*, **22**, 59-62.

600

601 KING L.H., & MACLEAN B. (1970). - Pockmarks on the Scotian shelf. *Geological Society of*  
602 *America Bulletin* **81**, 3141-3148.

603

604 KLUESNER J.W., SILVER E.A., BANGS N.L., MCINTOSH K.D., GIBSON J., & ORANGE D.  
605 (2013). - High density of structurally controlled, shallow to deep water fluid seep indicators imaged

606 offshore Costa Rica. *Geochemistry, Geophysics, Geosystems*, **14**(3), 519-39.

607

608 LAURENT M. (1993). – Datation par résonance de spin électronique (ESR) de quartz de formations  
609 quaternaires: comparaison avec le paléomagnétisme. Thèse, Muséum d'histoire naturelle et Université  
610 de Rennes1, 103p.

611

612 LEÓN R., SOMOZA L., MEDIALDEA T., HERNÁNDEZ-MOLINA F.J., VÁZQUEZ J.T., DÍAZ-  
613 DEL-RIO V., & FRANCISCO J. G. (2009). - Pockmarks, collapses and blind valleys in the Gulf of  
614 Cádiz. *Geo-Marine Letters*, **30**(3-4), 231-47.

615

616 LEÓN R., SOMOZA L., MEDIALDEA T., GONZÁLEZ F.J., GIMENEZ-MORENO C.J., & PÉREZ-  
617 LÓPEZ R. (2014). - Pockmarks on either side of the Strait of Gibraltar: formation from overpressured  
618 shallow contourite gas reservoirs and internal wave action during the last glacial sea-level lowstand?  
619 *Geo-Marine Letters*, **34**(2-3), 131-51.

620

621 MENIER D. (2003). - Morphologie et remplissage des vallées fossiles sud-armoricaines: apport de la  
622 stratigraphie sismique. Thèse de Doctorat d'État, Université de Bretagne Sud, p. 204.

623

624 MILLER D.J., KETZER J.M., VIANA A.R., KOWSMANN R.O., FREIRE A.F.M., & OREIRO S.G.  
625 (2015). - Natural gas hydrates in the Rio Grande Cone (Brazil): A new province in the western South  
626 Atlantic. *Marine and Petroleum Geology*, **67**, 187-96.

627

628 PICKRILL R.A. (1993). - Shallow seismic stratigraphy and pockmarks of a hydrothermally  
629 influenced lake, Lake Rototoiti, New Zealand. *Sedimentology* **40**, 813–828.

630

631 PILCHER R., & ARGENT J. (2007). - Mega-pockmarks and linear pockmark trains on the West  
632 African continental margin. *Marine Geology*, **244**, 15–32.

633



634 PINOT J.P. (1974). - Le pré-continent breton, entre Penmarc'h, Belle-île et l'escarpement continental,  
635 étude géomorphologique Bulletin de l'AFEQ3, **16**, 197-216.  
636

637 PROUST J.N., MENIER D., GUILLOCHEAU F., GUENNOC P., BONNET S., ROUBY S., & LE  
638 CORRE C. (2001). - Les vallées fossiles de la baie de Vilaine: nature et évolution du prisme  
639 sédimentaire côtier du Pleistocène armoricain. *Bulletin de la Société Géologique Française*, **172**(6),  
640 737-749.  
641

642 REYNAUD M., & BALTZER A. (2014). - Une association remarquable entre des crustacés  
643 amphipodes (*Haploops niraë*) et des pockmarks (cratères de dégazage naturels) en Baie de  
644 Concarneau. *Les cahiers Nantais*, 2014-2, 25-35.  
645

646 ROGERS J., KELLEY J.T., BELKNAP D.F., GONTZ A., & BARNARDT W. A. (2006). -  
647 Shallow water pockmarks formation in temperate estuaries: a consideration of origins in the western  
648 gulf of Maine with special focus on Belfast Bay. *Marine Geology*, **225** (1-4), 45-62.  
649

650 SCANLON K.M., & KNEBEL H. J. (1989). - Pockmarks in the floor of Penobscot Bay, Maine. *Geo-*  
651 *Marine Letters*, **9**, 53-58.  
652

653 SOURON A. (2009). - Sédimentologie des vasières subtidales à *Haploops* spp. sur les fonds à  
654 pockmarks de Bretagne Sud. Mémoire de Master 2 Sciences de la Mer et du Littoral, Université de  
655 Bretagne Occidentale, p. 53.  
656

657 USSLER III W., PAULL C.K., BOUCHER J., FRIEDERICH G.E., & THOMAS D.J (2003). -  
658 Submarine pockmarks: a case study from Belfast Bay, Maine, *Marine Geology*, **202**, 175-192.  
659

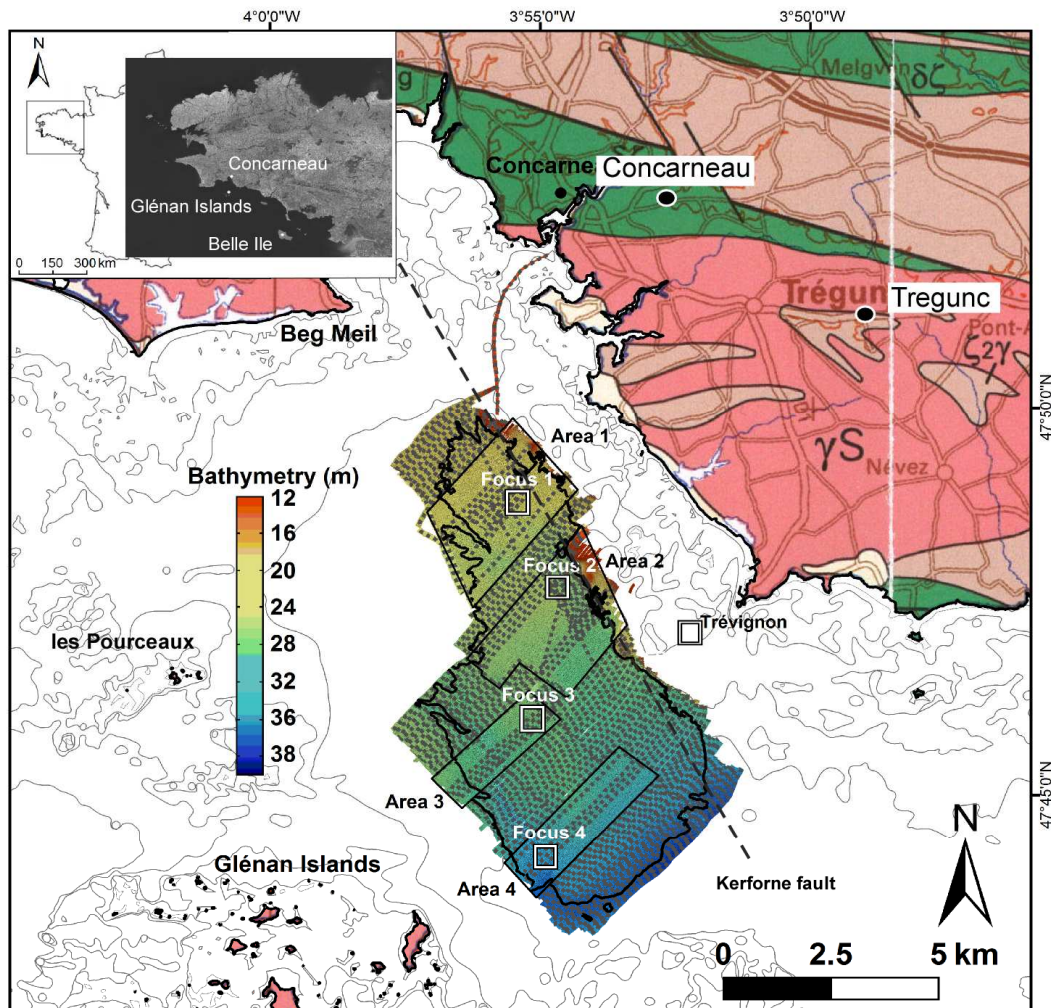
660 TESSIER C. (2006). - Caractérisation et dynamique des turbidités en zone côtière: l'exemple de la  
661 région marine Bretagne Sud., Thèse de Doctorat d'État, Université de Bordeaux, p. 323.

662

663 WESCHENFELDER J., KLEIN A.H.F., GREEN A.N., ALIOTTA S., MAHIQUESM.M., NETO  
664 A.A., TERRA L.C., CORREA I.C.S., CALLIARI L.J., MONTOYA I., GINSBERG S.S., & GRIEP  
665 G.H. (2016). - The control of palaeo-topography in the preservation of shallow gas accumulation:  
666 examples from Brazil, Argentina and South Africa., *Estuarine, Coastal and Shelf Science*, **172**, 93-  
667 107.

668

Figure 1



- Data acquired during Pock & Ploops (2011) : Areas 1, 2, 3 and 4
  - Data acquired during Pock & Tide (2014)
  - Haploops nirae* area limits
  - Selected focus 1, 2, 3 and 4 (profiles acquired in 2011 and 2014)
- Base map: 1/250 000 vectorised geological map from BRGM

Figure 2

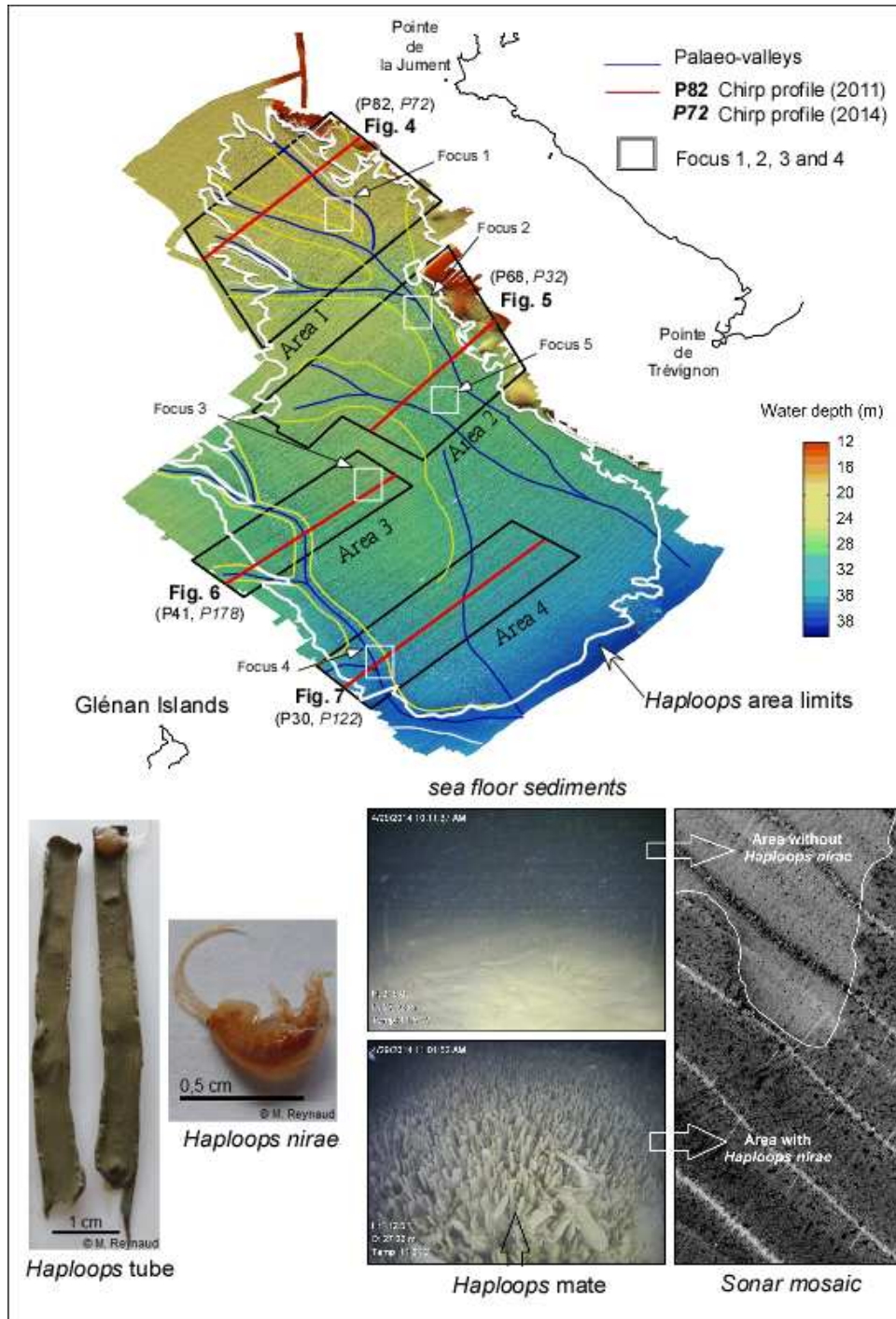




Figure 3

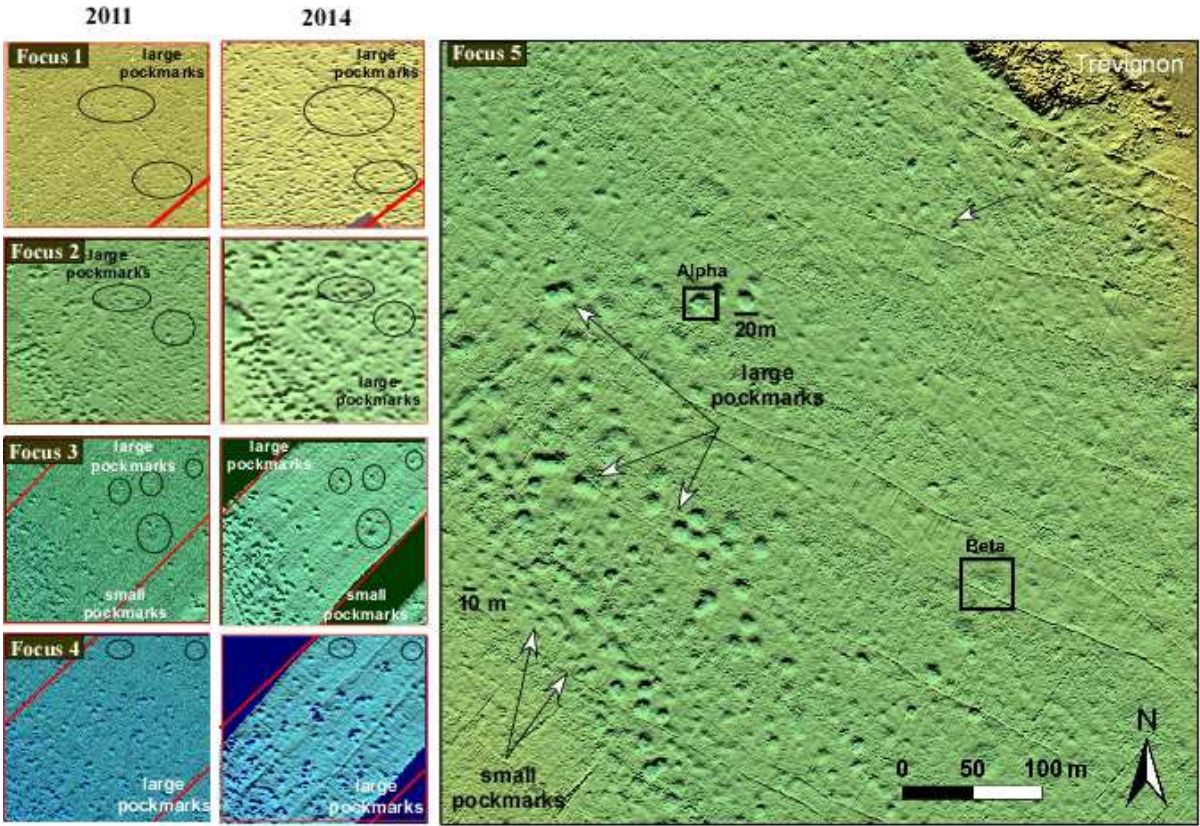


Figure 4

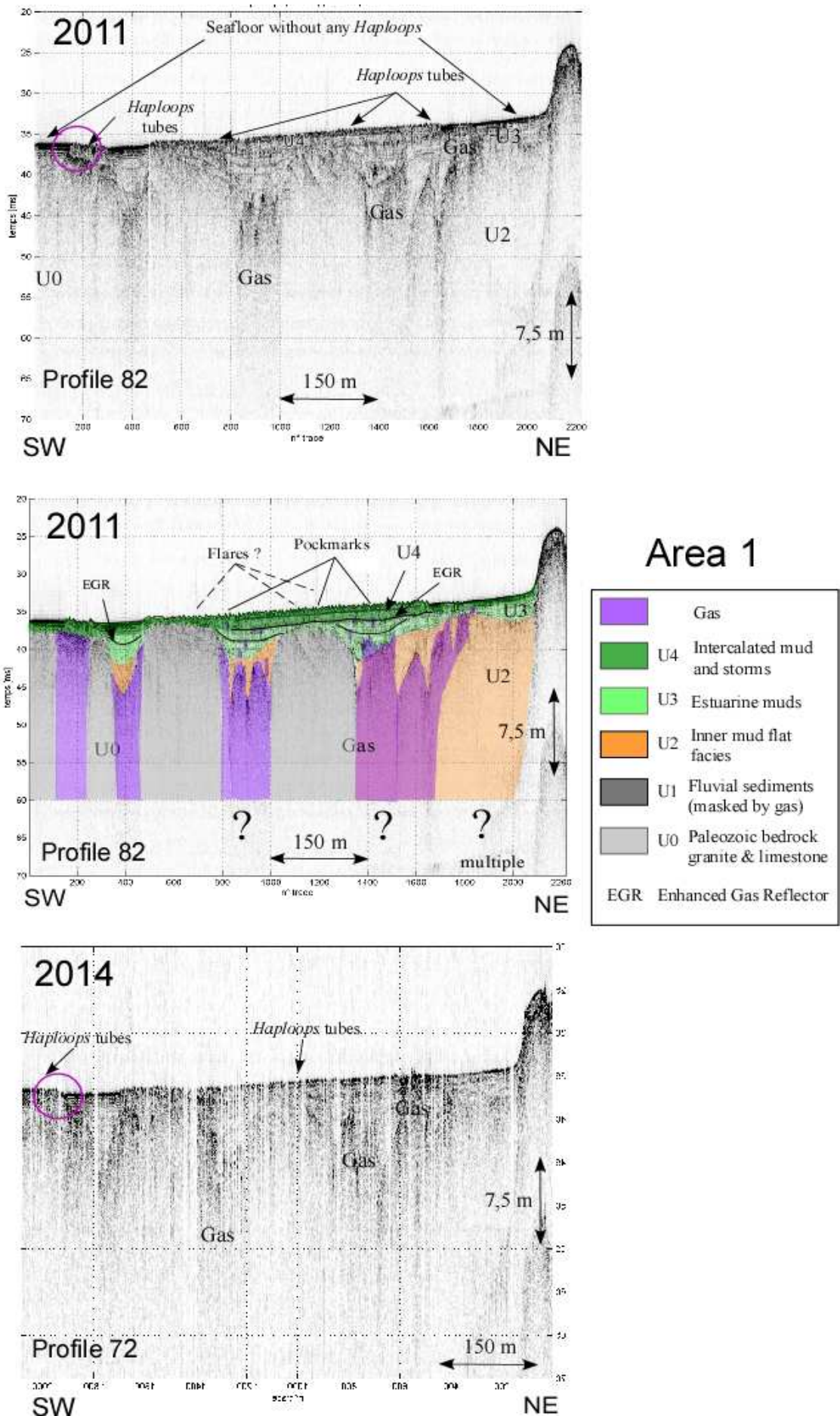
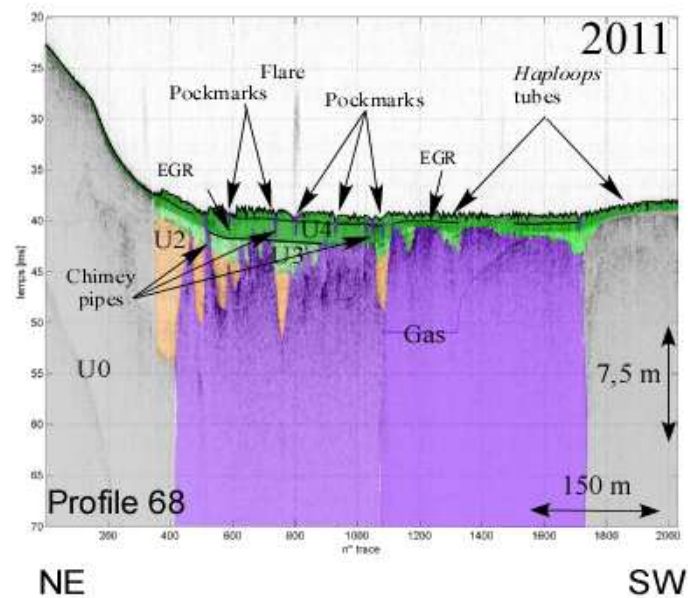
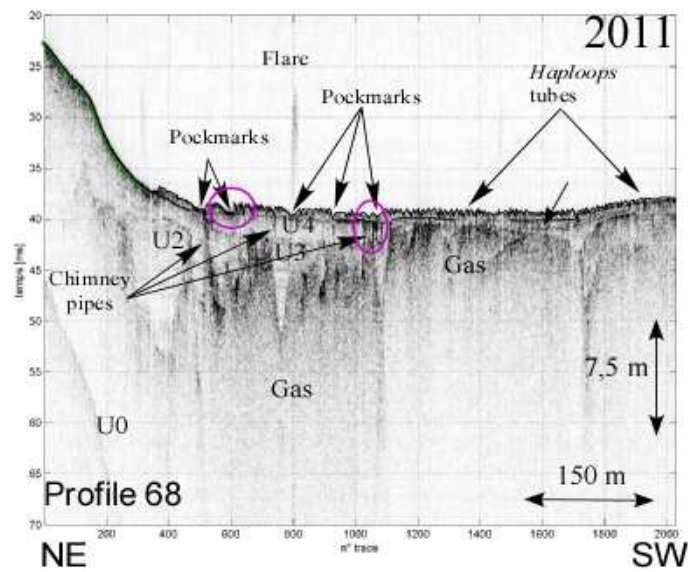




Figure 5



## Area 2

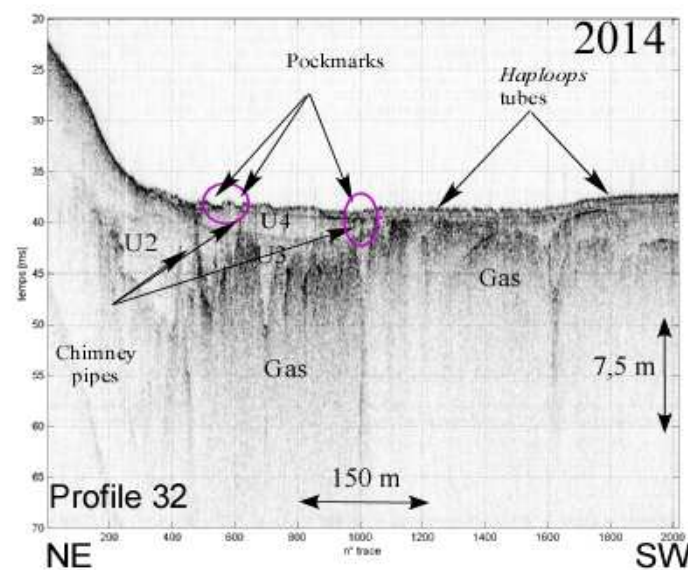
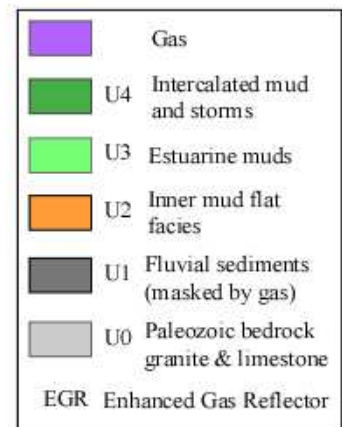


Figure 6

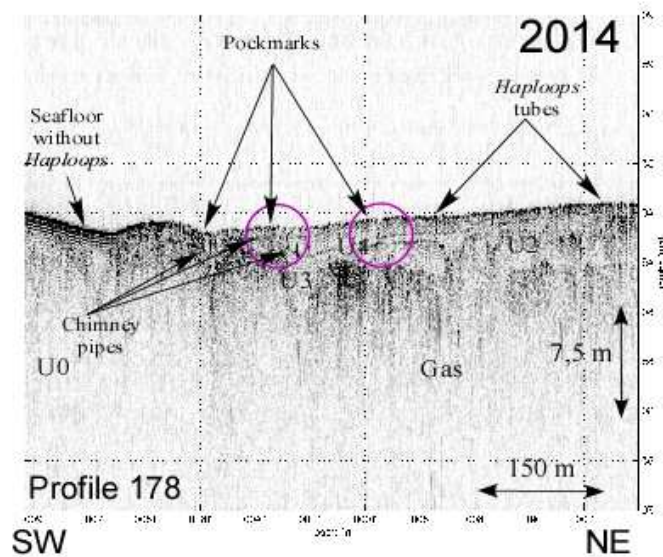
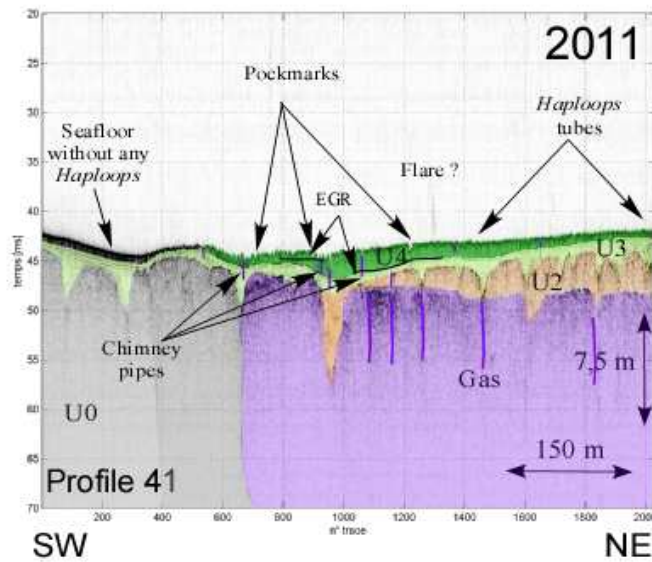
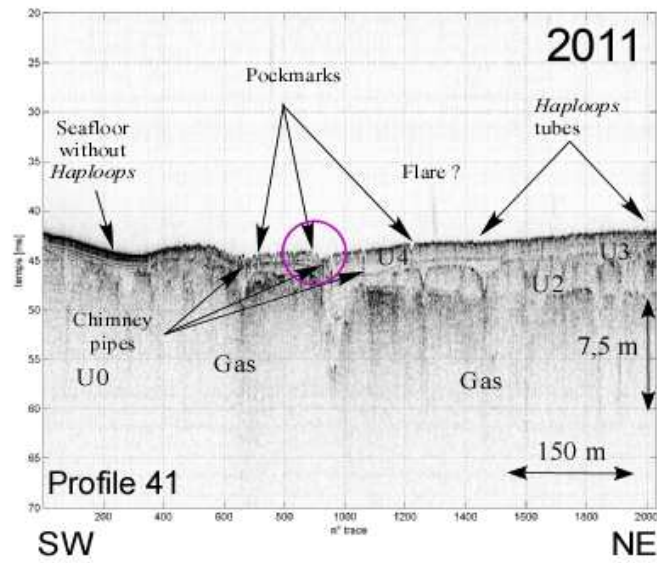




Figure 7

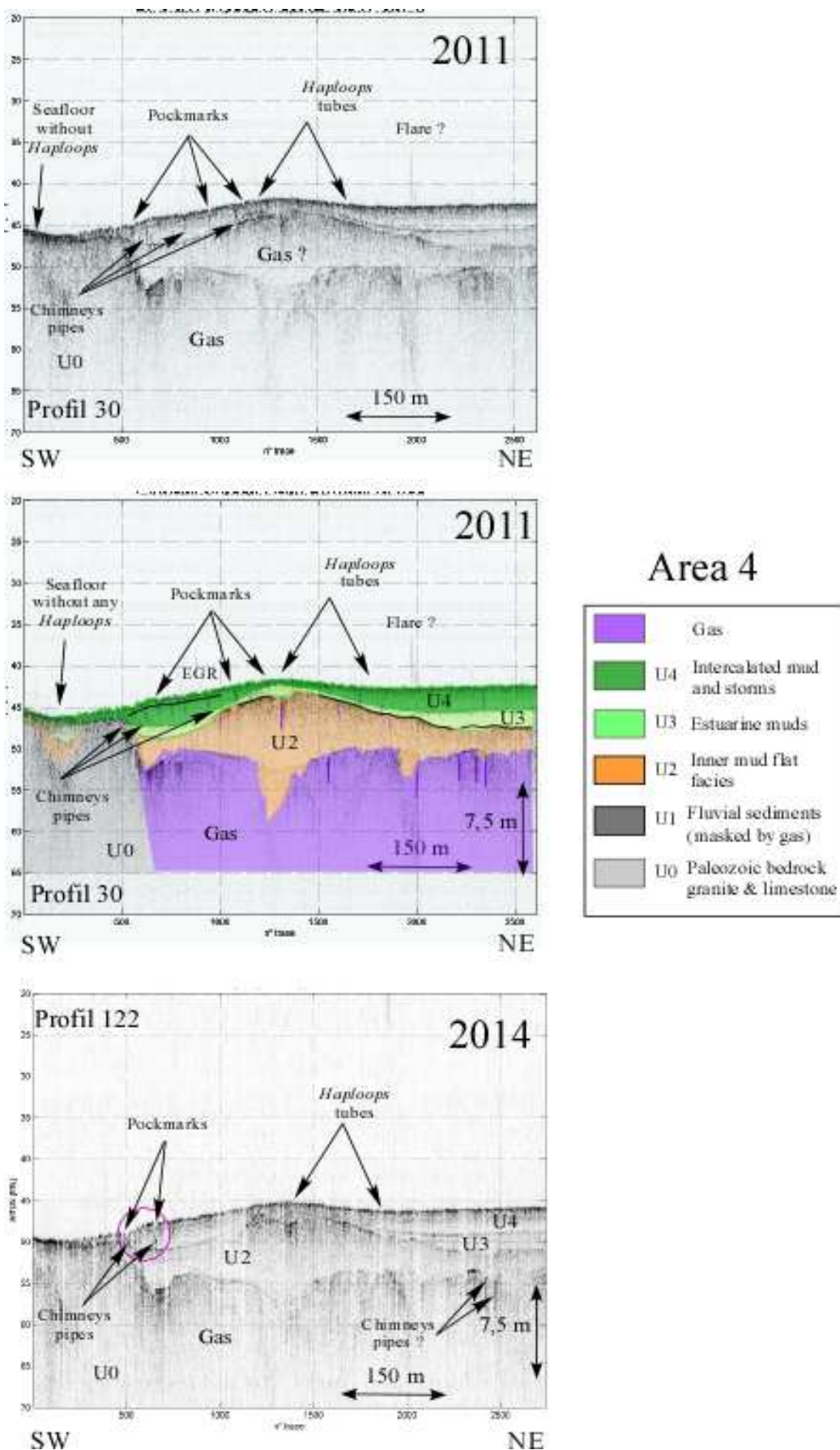


Figure 8

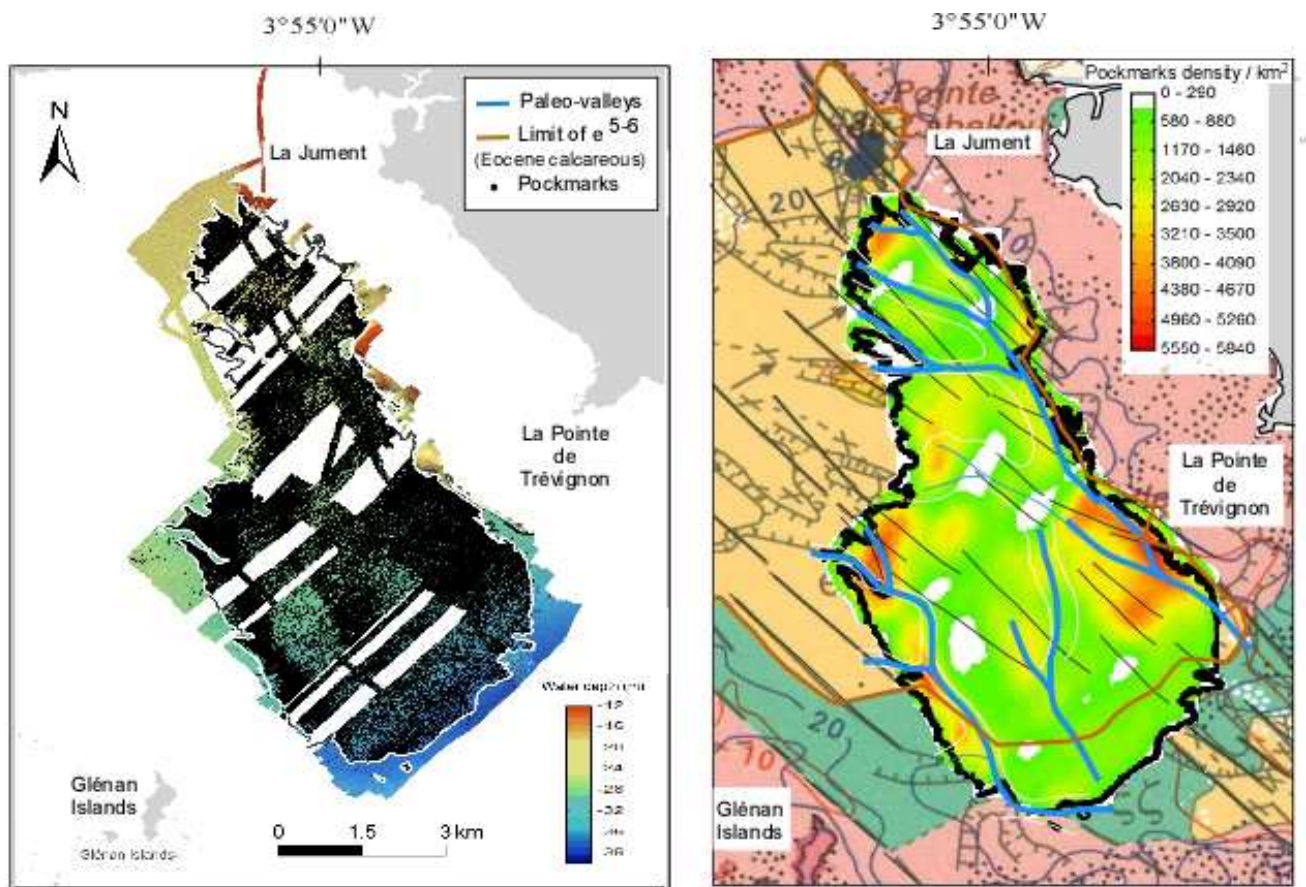


Figure 9

